Available online at www.sciencedirect.com
SCIENCE DIRECT®

Journal of the European Ceramic Society 23 (2003) 1517–1524

www.elsevier.com/locate/jeurceramsoc

Effects of Li_2O on the low temperature sintering and thermal conductivity of AlN ceramics

Liang Qiao[a,*], Heping Zhou[a], Kexin Chen[a], Renli Fu[b]

[a]*State Key Laboratory of New Ceramics and Fine Processing, Department of Materials Science and Engineering, Tsinghua University, Beijing, 100084, PR China*

[b]*College of Mechanical-Electronic and Material Engineering, China University of Mining and Technology, Jiangsu, Xuzhou, 221008, PR China*

Received 12 June 2002; accepted 22 September 2002

Abstract

Effects of Li_2O on the densification and the thermal conductivity of AlN ceramics sintered at a low temperature were studied by using Li_2CO_3, CaF_2 and Y_2O_3 as additives. DTA and XRD were employed to identify the formation of the liquid and the changes of the phase compositions during the sintering. SEM and TEM were used to observe the microstructures of AlN specimens sintered at 1650 °C. The results show that Li_2O is an effective sintering aid, leading to high densification and high thermal conductivity at low sintering temperatures. AlN specimens with full densification and thermal conductivity were achieved with Li_2O addition. The high densification comes from the promotion of the liquid containing Li and $CaYAlO_4$. The high thermal conductivity is attributed to the purification of the AlN lattice, the enhancement of the density and the elimination of some grain-boundary phases.

Keywords: AlN; Sintering; Thermal conductivity; Li_2O

1. Introduction

Aluminum nitride is considered to be a promising substrate and package material for high power integrated circuits because of its high thermal conductivity, low dielectric constant and thermal expansion coefficient close to that of silicon.[1–3] However, it is difficult to sinter due to the high covalent bonding. For full densification, rare-earth and/or alkaline earth oxides are often added as sintering aids in the fabrication of AlN ceramics.[4,5] These sintering aids not only help form the liquid phase that promotes the densification by the process of liquid-phase sintering, but also improve the thermal conductivity by decreasing the concentration of oxygen impurities in AlN lattice. In general, AlN ceramics with full densification and high thermal conductivity can be achieved at the high temperature (>1800 °C) using Y_2O_3 or CaO as additive.[6]

However, the high sintering temperature not only increases the production cost of AlN ceramics but also promotes significant grain growth, which results in a reduction of mechanical strength. It also limits the selection of the metals, which are used for the cofiring to the AlN multilayer substrates. Consequently the research in AlN ceramics is oriented towards achieving full densification at low sintering temperature. In this field, many studies[7–12] have been carried out. Watari et al.[11] achieved the thermal conductivity higher 170 W/m K using $LiYO_2$ and CaO as the sintering aids at 1600 °C for 6 h. Liu et al.[12] obtained the dense AlN ceramics with 187 W/m K at 1650 °C for 6 h by concurrent addition of CaF_2 and YF_3. Watari et al.[11] investigated the role of Li_2O in the densification of AlN ceramics sintered at 1600 °C. They found that Li_2O is an effective sintering aid because it decreases the temperature of the liquid occurrence and improves the wettability of the melt to AlN materials, thus promoting the densification of AlN. Also, the evaporation of Li_2O at 1600 °C purifies the grain boundaries, thus increasing the thermal conductivity of AlN ceramics. However, the effects of Li_2O on phase compositions, microstructure and thermal

* Corresponding author. Tel.: +86-10-6277-2550; fax: +86-10-6277-2549.
E-mail address: qiaoliang98@mails.tsinghua.edu.cn (L. Qiao).

0955-2219/02/$ - see front matter © 2002 Elsevier Science Ltd. All rights reserved.
PII: S0955-2219(02)00344-8

conductivity of AlN ceramics are not completely clear due to the lack of the experimental data. This paper used Li_2CO_3, CaF_2 and Y_2O_3 as additives to explore the effect of Li_2O on the sintering behavior and thermal conductivity of AlN ceramics sintered at a low temperature.

2. Experimental

Specimens were prepared through a conventional ceramic fabrication process. Commercially available AlN powder (grade US, Toyo Aluminium K. K.), as described in Table 1, was used as a starting material. The Li_2O additive was added in the form of Li_2CO_3 (analytical reagents) form. Powders of AlN with additives of Li_2CO_3, CaF_2 (analytical reagents) and Y_2O_3 (analytical reagents) were ball-milled by planetary milling for 2 h using ethanol as a mixing medium. The compositions of the specimens are shown in Table 2. After drying and binder-adding, the powder mixture was uniaxially die-pressed into pellets 10 mm in diameter and 5 mm thick and de-waxed at 550 °C. The pellets were then placed into a BN crucible and sintered at 1650 °C for 0, 2, 4, 6, 8 and 12 h respectively in a graphite furnace with a flowing nitrogen atmosphere.

Shrinkages and densities of the sintered pellets were measured by vernier caliper and Archimedes displacement method, respectively. The fracture surfaces of the pellets were observed by scanning electron microscopy (SEM, OPTON, CSM950) and transmission electron microscopy (JEM, 200CX). The thermal conductivity at room temperature was measured by a laser flash technique. To determine the lattice parameters, the samples with and without Li_2O sintered for 0, 4 and 8 h at 1650 °C were scanned from 90 to 140° at the rate of 0.1°/min using XRD with CuK_α radiation.

Table 1
Properties of the starting A1N powder

Chemical composition (wt.%)					Average particle size (pm)	Specific surface ($m^2\ g^{-1}$)
N	0	C	Si	Fe		
33.2	1.11	0.04	0.0059	0.0023	1.46	4.50

Table 2
Chemical compositions of the starting materials

	CaF_2 (wt.%)	Y_20_3 (wt.%)	Li_2CO_3 (wt.%)	$A1_20_3$ (wt.%)	A1N (wt.%)
CYA	2	2	0	0	96
CYAL	2	2	2	0	94
CYAO	30.8	30.8	0	38.4	0
CYAOL	23.5	23.5	23.5	29.5	0

In Sample CYAO and Sample CYAOL, Al_2O_3 was added in the additives as one of the reactants to examine the phases in the sintering. Those samples were annealed at different temperatures and then characterized by XRD. In order to understand the formation of the liquid in the sintering, CaF_2–Y_2O_3–Al_2O_3 and CaF_2–Y_2O_3–Al_2O_3–Li_2CO_3 systems were studied by differential thermal analysis (PYRIS DTA7). The analysis was carried out in an N_2 ambient at a heating rate of 5 °C/min from room temperature to 1500 °C.

3. Results

3.1. Shrinkage

The shrinkages of samples CYA and CYAL sintered at different temperatures are shown in Fig. 1. The larger shrinkage of Sample CYAL implies Li_2O promotes the densification in sintering. Especially, Sample CYAL has a very quick shrinkage within the range 1450–1600 °C. After sintered at 1650 °C for 12 h, Sample CYAL obtains a shrinkage of 18.6%.

3.2. DTA

Fig. 2 shows the DTA curves of samples CYAO and CYAOL. In the curve of Sample CYAO, the obvious endotherms occur near 1400 °C. The endotherm at 1402 °C associates with the melting of CaF_2 and that at 1384 °C probably with partial reactions between the additives. In the case of Li_2O addition, besides the endotherm at 1398 °C associated with the melting of CaF_2, three endotherms occur at about 1055, 1105 and 1286 °C respectively. This implies that some reactions can occur between the additives at lower temperatures in the presence of Li_2O.

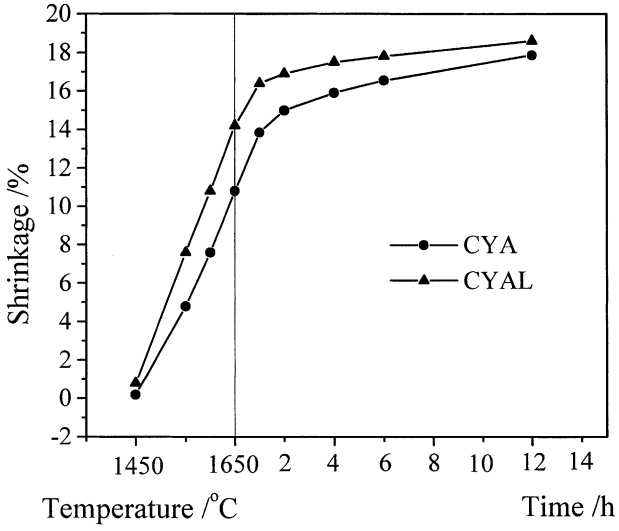

Fig. 1. Shrinkages of samples CYA and CYAL.

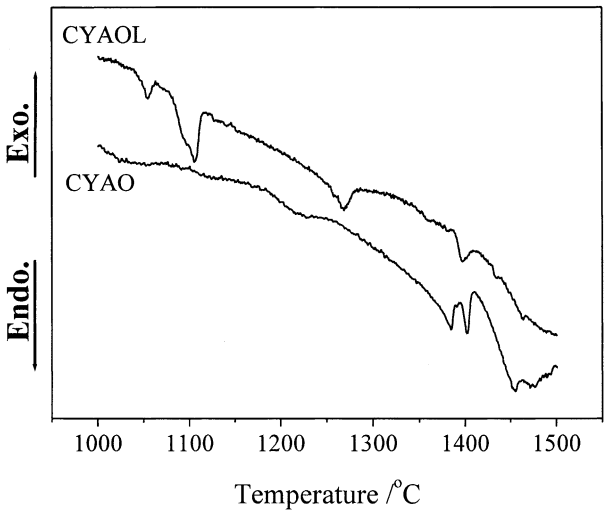

Fig. 2. DTA curves of samples CYAO and CYAOL.

3.3. Phase compositions

The phases of different systems are summarized in Table 3. The phase composition in Sample CYAOL is different from that in Sample CYAO. At 950 °C, trace of YAM ($Y_4Al_2O_9$) forms in the system of CaF_2–Y_2O_3–Al_2O_3, but in the presence of Li_2CO_3, phase γ-$LiAlO_2$ appears besides YAM, which comes from the reaction between Al_2O_3 and Li_2O formed by the decomposition of Li_2CO_3 as follows:

$$Li_2CO_3 = Li_2O + CO_2 \quad (1)$$

$$Li_2O + Al_2O_3 = 2LiAlO_2 \quad (2)$$

In Sample CYAO annealed at 1100 °C, phases YAM, YAP ($YAlO_3$), $CaYAl_3O_7$ and $Ca_{12}Al_{14}F_2O_{32}$ are identified, which indicates that CaF_2 and Y_2O_3 react with Al_2O_3 at this temperature. Since Y_2O_3 has a low reaction temperature with Al_2O_3, it is possible that the amount of Y_2O_3 influences the formation of the Ca–Al–O compounds due to the consumption of Al_2O_3. In the presence of Li_2O, the amounts of the Ca–Al–O compounds in Sample CYAOL are so small that they are undetectable. This is probably attributed to a loss of Al_2O_3, which reacts with Li_2O and Y_2O_3 to form γ-$LiAlO_2$, YAM and $CaYAl_3O_7$ considering that a large quantity of CaF_2 and only traces of Al_2O_3 remain in the fired powder. When the temperature increases to 1650C, phases $Ca_{12}Al_{14}O_{33}$ and $Ca_2Al_2O_5$ occur in Sample CYAO, but no Ca-Al-O compounds are identified in Sample CYAOL. It is noted that the Al_2O_3-rich phase, YAG, is formed in Sample CYAOL at 1650 °C, which implies an increase of the amount of Al_2O_3. In samples CYA and CYAL sintered for 8 h, phase $CaYAlO_4$ is identified, while the peaks of $CaYAl_3O_7$ become weak.

Using XRF, the element contents of Ca and Y in samples CYA and CYAL sintered at 1650 °C were detected. As shown in Fig. 3(a), the Ca content decreases in sample CYA with the increasing soaking time, which may be associated with the evaporation of Ca–Al–O compounds in a carbon-containing nitrogen atmosphere, as described by Greil et al.[13] After 6-h sintering, the decrease of the Ca content becomes very slow, which implies that $CaYAlO_4$ is stably remained in the sample. Different from the change in sample CYA, the Ca content in sample CYAL has a very small reduction during the whole sintering, which is associated with the lack of the evaporation of Ca–Al–O compounds and the stable existence of phase $CaYAlO_4$. The content of element Y decreases with increasing the sintering time in both Sample CYA and Sample CYAL, which is supposed to result from the migration of the liquid containing yttrium from the interior to the surface of the sintered specimens. This is also the reason why the Y/Al ratio is greater than the chemical compositions in Fig. 3(b) since the measured surface is close to the natural surface. It is noted that the changes of Ca and Y contents in samples CYA and CYAL sintered from 6 to 12 h have the similar trajectory, which implies that the samples with and without Li_2O have similar phases after a long sintering, consistent with the XRD results as shown in Table 3.

3.4. Microstructure

The microstructures of the fracture surfaces of samples CYA and CYAL sintered for different time are shown in Fig. 4. From the photographs, it is observed that in sample CYAL, the liquid homogeneously distributes when the temperature reaches 1650 °C, which indicates the redistribution of the liquid ends before this temperature. This is different from the change of microstructure of the sample with CaF_2–Y_2O_3 addition.[14] As shown in Fig. 5, the dihedral angles are about 120° between the polyhedral grains with small amounts

Table 3
Phase compositions of different samples

	CYAO	CYAOL
950 °C for 1 h	CaF_2, Y_2O_3, $A1_2O_3$, trace of YAM	Y_2O_3, CaF_2, YAM, $CaYA1_3O_7$, λ-$LiAlO_2$
1100 °C for 1 h	CaF_2, $Ca_{12}A1_{14}F_2O_{32}$, $Y_4Al_2O_9$, $YAIO_3$, $CaYAI_3O_7$	CaF_2, $Y_4A1_2O_9$, $CaYAI_3O_7$, y-L1AIO$_2$, trace of Y_2O_3
1650 °C for 0 h	$Y_4A1_2O_9$, $Ca_{12}Al_{14}O_{33}$, $Ca_2A1_2O_5$, $CaYA1_3O_7$, trace of $CaYAIO_4$	$Y_4A1_2O_9$, $Y_3A1_5O_{12}$, $CaYA1_3O_7$, trace of $CaYAIO_4$
1650 °C for 8 h	$Y_4A1_2O_9$, $CaYA1O_4$, trace of $CaYAI_3O_7$,	$Y_4A1_2O_9$, $CaYA1O_4$, trace of $CaYA1_3O_7$

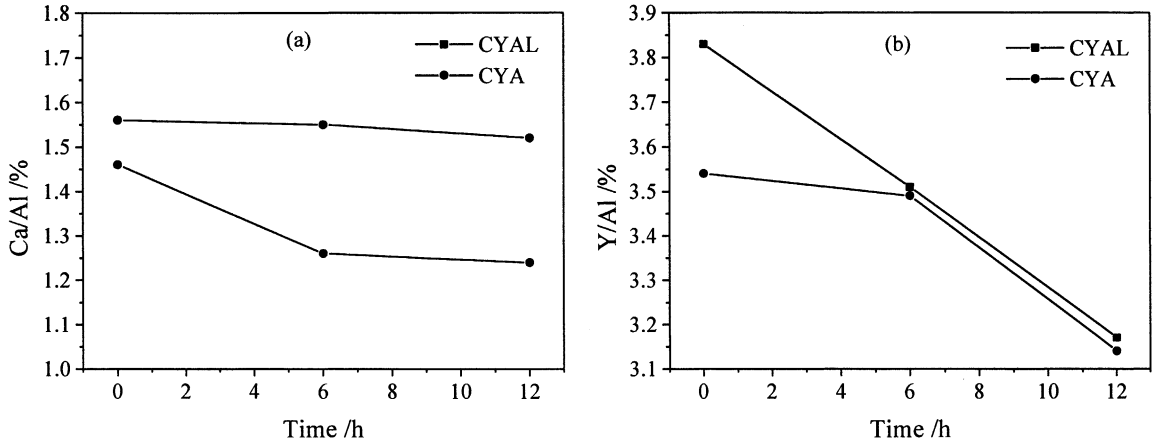

Fig. 3. Contents of Ca and Y in samples CYA and CYAL sintered at 1650°C: (a) Ca/Al and (b) Y/Al.

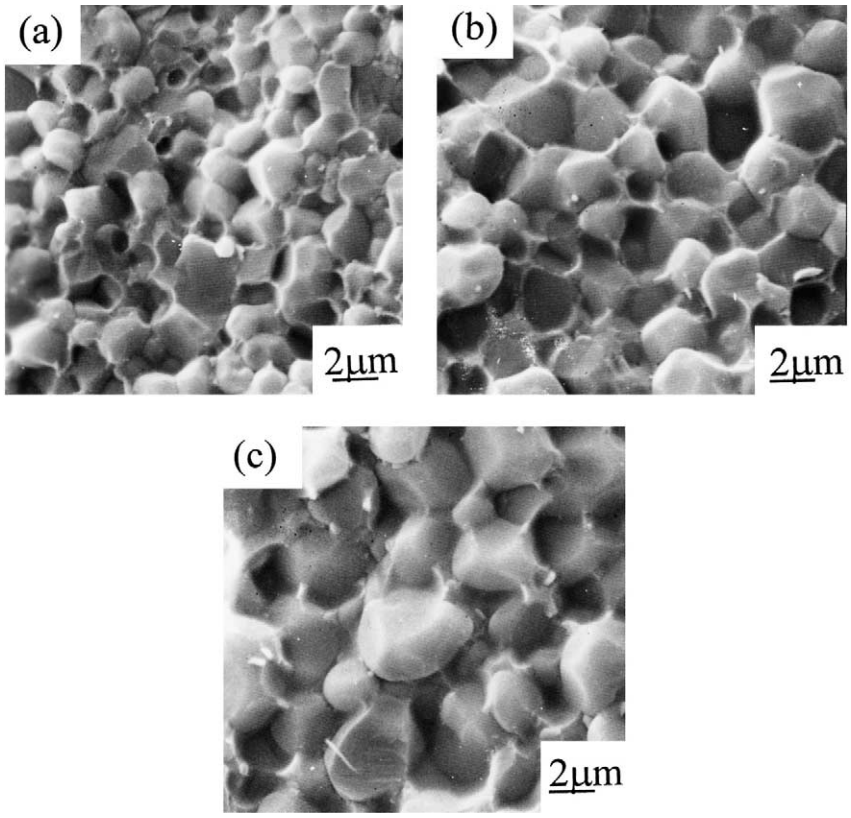

Fig. 4. Microstructures of Sample CYAL sintered at 1650°C for (a) 0 h, (b) 6 h, and (c) 12 h by SEM.

of grain-boundary phases at the three-grain junctions in Sample CYA, which implies the less wetting of the grain boundary phases to the AlN grains. However, the dihedral angle less than 60° between the grains in Sample CYAL shows the good wettability of the liquid phases. The selected area electron diffraction patterns in Sample CYAL show that three phases are contained in the liquid field as shown in Fig. 5(b). The regular spots and the diffractive rings show the existence of phase YAM and some polycrystalline phase in the sample. Besides the two crystalline phases, the clear dispersive ring ("halo") in the micrograph indicates that some glass phase exists in the liquid field, which is predicted to be the sources of the differences in shrinkage and thermal conductivity.

3.5. Thermal conductivity

The qualitative information about the oxygen concentration in the AlN lattice and, indirectly, of its thermal conductivity is obtained by the careful determination of the AlN lattice parameters. A reduction

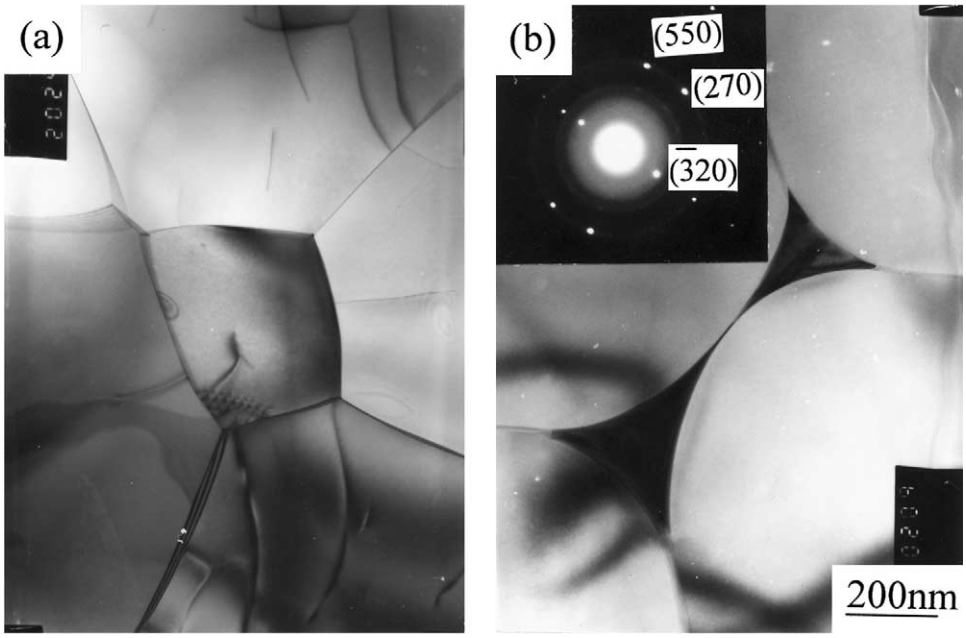

Fig. 5. TEM of samples (a) CYA and (b) CYAL sintered at 1650 °C for 4 h.

of the *c* lattice parameter corresponds to higher oxygen concentration and lower thermal conductivity of the AlN grains..[1,15] Table 4 shows the lattice parameters, densities and thermal conductivities of samples CYA and CYAL. From the table, it is observed that the densities and the thermal conductivities of samples CYA and CYAL increase during sintering. The thermal conductivities of Sample CYAL are much higher than those of Sample CYA when sintered at same conditions. In Sample CYA, the length of *c*-axis has no change with the sintering time, which implies the increase of the thermal conductivity mainly comes from the enhancement of the densification. In Sample CYAL, the length of *c*-axis increases from 4.9790 to 4.9794 Å when sintered from 0 to 4 h. This implies that the increasing thermal conductivity in this stage is probably attributed to the increase of the density and the purification of the AlN lattice. Though the density and *c*-axis length of the sample sintered for 8 h have small changes compared with that for 4 h, the thermal conductivity still greatly improves, which may result from the evaporation of some grain-boundary phases after a long sintering.

Table 4
Lattice parameter, unit cell volume, density and thermal conductivity of sintered A1N at 1650 °C

Sample	*a* (Å)	*c* (Å)	Unit cell volume (Å^3)	Density (g/cm^3)	Thermal conductivity (W/m K)
CYA for 0 h	3.1119	4.9790	41.755	3.01	109
CYA for 4 h	3.1118	4.9789	41.752	3.24	137
CYA for 8 h	3.1118	4.9788	41.751	3.26	148
CYAL for 0 h	3.1120	4.9790	41.758	3.19	122
CYAL for 4 h	3.1120	4.9794	41.761	3.24	147
CYAL for 8 h	3.1120	4.9793	41.760	3.26	167

4. Discussion

4.1. Effect on phase compositions

In general, three yttrium aluminates can be formed by the reaction between Y_2O_3 and Al_2O_3. The grain-boundary phase with YAM ensures the purification of the AlN lattice, and thus, the attainment of high thermal conductivity due to the low activity of oxygen in it.[16] Since a large amount of Y_2O_3 benefits the formation of YAM, the amount of Y_2O_3 added should not be too small from the point of purifying AlN lattice. However, a large amount of YAM, as the solid grain-boundary phase at temperatures below 1650C, slows down the densification of AlN ceramics.[14] Hence only a proper amount of Y_2O_3 can result in AlN ceramics with high thermal conductivity.

Li_2O has a great effect on the densification of changing the phase compositions of the liquid in AlN ceramics during sintering. Because of the consumption of Al_2O_3 by the formation of γ-$LiAlO_2$, YAM and $CaYAl_3O_7$ at 950 °C, Ca–Al–O compounds are difficult to form, which makes it impossible to promote the densification by forming the calcium aluminates liquid in the sample with Li_2O. When the temperature increases to 1100 °C, the mixed powders containing Li_2O are

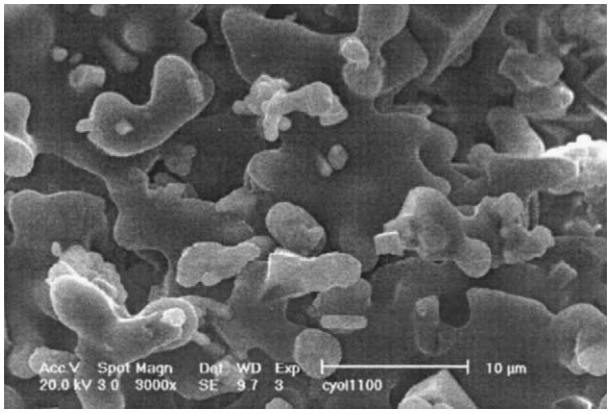

Fig. 6. SEM of Sample CYAOL sintered at 1100°C for 1 h.

covered with a layer of liquid as shown in Fig. 6, which corresponds to the earlier and greater shrinkage below 1650 °C in the sample with Li_2O compared with that without it as shown in Fig. 1. In the previous study,[16] the densities of AlN specimens increase from 1300 °C, which also probably comes from the promotion of this liquid. As shown in Fig. 1, the sample with Li_2O addition shrinks 0.8%, while the sample without it nearly keeps the original size at 1450 °C.

As Watari et al.[11] summarized, $LiAlO_2$ has a high Gibbs energy (−779 KJ/mol at 1530 °C) in aluminates, which makes it easily decompose into Li_2O and Al_2O_3 above this temperature. The evaporation of Li_2O with the high vapor pressure (>10Pa at 1600 °C) avoids the problems associated with residual sintering aids in the grain boundaries, which can influence the electrical resistivity of AlN specimens and lead to morphological changes on the surface of AlN substrates during metallization processes.[11] Al_2O_3 results in the formation of phase YAG at 1650 °C as shown in Table 3. As a result, different from the promotion of the liquid calcium aluminates and $CaYAlO_4$ liquid on the densification of Sample CYA,[14] the shrinkage in the sample with Li_2O addition is mainly associated with the action of the liquid containing Li and $CaYAlO_4$. Since there are the same phases present in samples CYA and CYAL after long sintering, the contents of Ca and Y have the similar change trajectory in these two samples as shown in Fig. 3.

4.2. Effect on sintering behavior

The shrinkage-time trajectories from the sample with and without Li_2O are shown in Fig. 7(a). Samples CYA and CYAL yield a linear trajectory between log ($\Delta L/L_0$) and log t. The slopes of the two lines are much lower than 1/3, i.e., 0.05 for sample CYAL and 0.1 for CYA respectively. This implies that solution-precipitation probably occurs before the sintering at 1650 °C according to the theory of liquid phase sintering.[17] As shown in Fig. 4, liquid homogeneously distributes in Sample CYAL during the whole sintering. Thus, the sintering probably has entered the stage of grain growth in Sample CYAL when the temperature arrives at 1650 °C, while the rearrangement of some particles with the redistribution of the liquid may still occur in sample CYA,[14] which produces the higher slope but lower starting shrinkage in sample CYA compared with that in CYAL.

From the results of the linear fit to the experimental data, the shrinkages of samples CYA and CYAL vs time during the sintering follow the equation:

$$\Delta L/L_0 = -At^{\alpha} \quad (3)$$

where constants $A=0.1085$ and $\alpha=0.05$ for sample CYAL; and $A=0.0613$ and $\alpha=0.1$ for Sample CYA. The trajectories are plotted as shown in Fig. 7(b). If shrinkage follows Eq. (3) during the whole sintering, the sintering time needed will be 25.3 h when Sample CYA has the same shrinkage of 19.2% with Sample CYAL. Since the shrinkage generally becomes slower at the end of the sintering, it is almost impossible that the shrinkage of the sample without Li_2O exceeds that of Sample CYAL in a short sintering often used. Thus, the early and quick shrinkage before 1650 °C in the presence of Li_2O produces prominent advantage on the final shrinkage of AlN specimens.

4.3. Effect on thermal conductivity

The surface of AlN particles is supposed to be covered with a homogeneous layer of oxygen. The additives cannot contact all the oxygen and react with it since they are solid particles. This is why phase YAM is still formed even in the case of Y_2O_3/Al_2O_3 (mol) <2, as shown in Table 3. Because the inhomogeneous liquid distribution till 1650 °C results in the incomplete reaction between Y_2O_3 and Al_2O_3 in Sample CYA,[14] the remaining oxygen on the surface of the AlN particles diffuses into the AlN lattice to form oxygen-related defects at 1650 °C. During sintering, the effect of the liquid on the removal of the oxygen from the lattice to the surface is not prominent since the grain-boundary phases move to the three-grain junctions, which makes the removal of the oxygen from the lattice to the surface difficult. In the case of Li_2O addition, due to the formation of the liquid containing Li at about 1100 °C, the solids CaF_2 and Y_2O_3 have a close contact with the AlN particles with the flowing liquid, which benefits the reaction between them and the oxygen on the surface of particles, thus decreasing the oxygen content directly covering on the surface of the AlN particles. During the sintering at 1650 °C, the liquid with YAM has an effective wetting to the AlN grains, which enhances the removal of the oxygen from the lattice to the surface,

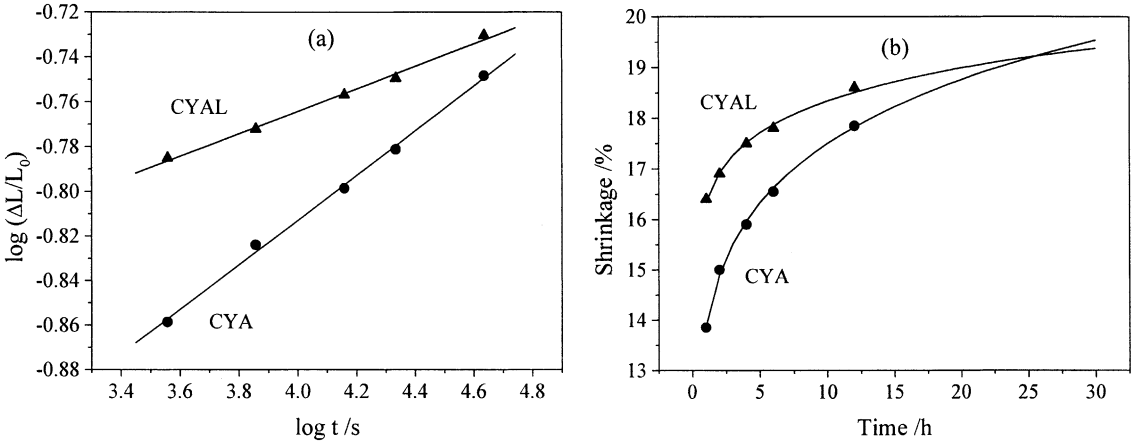

Fig. 7. Plot of shrinkage vs sintering time for samples CYA and CYAL: (a) log-shrinkage vs log-time and (b) shrinkage vs time.

thus increasing *c*-axis and the thermal conductivity as shown in Table 4. When the sintering time is long enough, the decomposition of the liquid containing Li and the transformation from phase $CaYAl_3O_7$ to $CaYAlO_4$ release some amount of Al_2O_3, which limits the increase of the c-axis length of the sample sintered for 8 h. Thus, the higher thermal conductivity of Sample CYAL mainly comes from the enhancement of the densification and the evaporation of some grain-boundary phases.

Li_2O significantly promotes the purification of AlN lattice during sintering as discussed above. However, the grain boundary phases in Sample CYAL deteriorates its thermal conductivity. As summarized by Harris et al.,[18] the AlN unit cell volume, as determined by X-ray diffraction measurements, as a function of sample thermal conductivity is shown in Fig. 8. It can be seen that the thermal conductivities of Sample CYA and Sample CYAL sintered for 8 h have a good consistence with the curve, which indicates the slight effect of the grain boundary phases on them. However, the thermal conductivities of Sample CYAL sintered for 4 and 8 h, which have a high unit cell volume and a high density, are much lower than the curve due to a large amount of grain boundary phases.

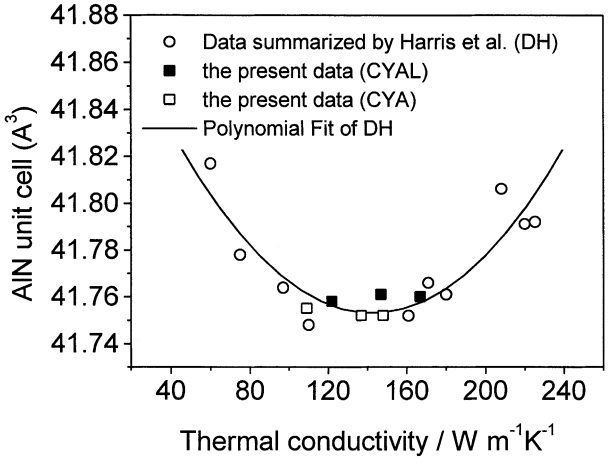

Fig. 8. AlN unit cell volume, as determined by X-ray diffraction measurements, as a function of thermal conductivity. The curve is a polynomial fit from the data summarized by Harris et al.[18]

5. Conclusions

Li_2O has important effects on the low temperature sintering and the thermal conductivity of AlN ceramics. The liquid containing Li formed at about 1100 °C decreases the starting temperature of the shrinkage of AlN ceramics and liquid $CaYAlO_4$ promotes the densification of AlN ceramics during the middle and final stages of sintering at 1650 °C. This produces a higher shrinkage and density in the sample with Li_2O addition. Li_2O not only benefits the formation of YAM and $CaYAlO_4$ but also makes the liquid phase effectively wet to the AlN particles, which leads to a purification of AlN lattice at a low sintering temperature, and thus ensures a high thermal conductivity. As a disappearing sintering aid, Li_2O also purifies the grain boundaries of AlN ceramics and hence avoids the contamination of AlN associated with it.

Acknowledgements

The authors wish to express their appreciation to Prof. X. Zhang and Dr. Y. Liu for the helpful discussions in this paper.

References

1. Slack, G. A., Nonmetallic crystals with high thermal conductivity. *J. Phys. Chem. Solids*, 1973, **34**, 321–335.
2. Sheppard, L. M., Aluminum nitride: a versatile but challenging material. *Am. Ceram. Bull.*, 1990, **69**(11), 1801–1803.

3. Baik, Y. and Drew, R. A. L., Aluminum nitride: processing and applications. *Key Eng. Mater.*, 1996, **122–124**, 553–570.
4. Komeya, K., Inoue, H. and Tsuge, A., Role of Y_2O_3 and SiO_2 additions in sintering of AlN. *J. Am. Ceram. Soc.*, 1974, **54**, 411–412.
5. Komeya, K., Tsuge, A. and Inoue, H., Effect of $CaCO_3$ addition on the sintering of AlN. *J. Mater. Sci. Lett.*, 1986, **1**, 325–326.
6. Huseby, I. C. and Bobik, C. F. US Patent 4,547,471, 1985.
7. Hashimoto, N., Yoden, H. and Deki, X., Sintering behavior of fine aluminum nitride powder synthesized from aluminum polynuclear complexes. *J. Am Ceram. Soc.*, 1992, **75**(8), 2098–2106.
8. Liu, Y., Zhou, H., Wu, Y. and Qiao, L., Improving thermal conductivity of aluminum nitride ceramics by refining microstructure. *Mater. Lett.*, 2000, **43**, 114–117.
9. Troczynski, T. B. and Nicholson, P. S., Effect of additives on the pressureless sintering of aluminum nitride between 1500°C and 1800 °C. *J. Am. Ceram. Soc.*, 1989, **72**(8), 1488–1491.
10. Jarrige, J., Bouzouita, K., Doradoux, C. and Billy, M., A new method for fabrication of dense aluminium nitride bodies at a temperature as low as 1600°C. *J. Eur. Ceram. Soc.*, 1993, **12**, 279–285.
11. Watari, K., Hwang, H. J., Toriyama, M. and Kanzaki, S., Effective sintering aids for low-temperature sintering of AlN ceramics. *J. Mater. Res.*, 1999, **14**(4), 1409–1417.
12. Liu, Y., Zhou, H., Qiao, L. and Wu, Y., Low-temperature sintering of aluminum nitride with YF_3-CaF_2 binary additive. *J. Mat. Sci. Lett.*, 1999, **18**, 703–704.
13. Greil, P., Kulig, M. and Hotza, D., Aluminum nitride ceramics with high thermal conductivity from gas-phase synthesized powders. *J. Eur. Ceram. Soc.*, 1994, **13**, 229–237.
14. Qiao, L., Zhou, H., Xue, H. and Wang, S., Effect of Y_2O_3 on low temperature sintering and thermal conductivity of AlN ceramics. *J. Eur. Ceram. Soc.*, 2003, **23**(1), 61–67.
15. Baranda, P. S., Knudsen, A. K. and Ruh, E., Effect of CaO on the thermal conductivity of aluminum nitride. *J. Am. Ceram. Soc.*, 1993, **76**(7), 1751–1760.
16. Jackson, T. B., Virkar, A., More, K. L., Dinwideie, R. B. and Cutler, R. A., High-Thermal-conductivity aluminum nitride ceramics: the effect of thermodynamic, kinetic, and microstructural factors. *J. Am. Ceram. Soc.*, 1997, **80**(6), 1421–1435.
17. Rahaman M. N. Ceramic Processing and Sintering. Marcel Dekker, 1995, p. 515.
18. Harris, J. H., Youngman, R. A. and Teller, R. G., On the nature of the oxygen-related defect in aluminum nitride. *J. Mater. Res.*, 1990, **5**, 1763–1773.